

PROTOTYPE OF THE DLR OPERATIONAL COMPOSITE CLOCK: METHODS AND TEST CASES

Matthias Suess and Jens Hammesfahr
E-mail: *Matthias.suess@dlr.de*
German Aerospace Centre (DLR)
Oberpfaffenhofen, Germany

Abstract

The operational implementation of the ensemble Kalman filter Composite Clock (CC developed by K. R. Brown), is the subject of this paper. Although the mathematical background of the CC is well-known, its autonomous and robust operation in a clock laboratory requires further modifications of the CC. The suitable initialization of the first ensemble estimate is discussed. Due to the fact, that only difference measurements are available, there is a dimensional degree of freedom in the first as in the following ensemble estimates. Furthermore, to guarantee a robust, consistent, and autonomous estimation of the ensemble clocks, a consistency check is described. It outputs a so-called consistency matrix which describes the active and non-active clocks. Since the identified active clocks can change from measurement to measurement, the corresponding Kalman filter (KF) parameters are adapted in a consistent way. Finally, the non-active clocks are estimated based on the KF output. The performance of the OCC using an ensemble of five DLR laboratory clocks, measured over a period of 1 year, is outlined. The clock ensemble consists of three high-performance cesium-clocks (HP5071A), an active H-maser (CH1-75), and a GPS-disciplined Rb clock. Although miscellaneous anomalies like phase steps, outliers, and clock exclusions arise, the OCC autonomously processes the five ensemble clocks and establishes a robust system time. Analysis results of this ensemble with different types of clocks when applying the OCC are presented.

SYSTEM TIME CONCEPTS FOR GNSS

Besides orbits and other system parameters, a Global Navigation Satellite System (GNSS) generates and provides satellite clock offsets to the users. The clock or time offsets are with respect to (w.r.t.) the GNSS system time (ST). It is an integral part of the GNSS and is a key element of the GNSS performance.

There can be extracted three requirements on the system time:

1. Stability of ST: no impact on satellite clocks for any τ value
2. Robustness of ST: stability is guaranteed at any time t
3. Metrology of ST: representation of UTC and long-term performance.

Regarding the ST implementation which shall provide the listed requirements, there can be distinguished two concepts.

The first ST concept is based on a *master clock*. The system time is established by a highly stable atomic clock, e.g. an active hydrogen maser. Its short-term stability of about $2 \times 10^{-13} @ 1$ s generally fulfills the first requirement. However, to meet the second requirement, “robustness,” the master concept has to deal with master clock failures like outage, time or frequency steps, or outliers. A steered backup master clock can be installed to solve these issues. In case of a detected master clock failure, the system time is established by the backup clock. The challenge is to provide such additional hardware and technology to steer the backup clock. Similarly, the third requirement is fulfilled by steering the master clock w.r.t. UTC.

The second ST concept is based on *ensemble time*. The system time has got no physical representation and is computed by a timescale algorithm ([1]), which computes the time offsets of the ensemble clocks to the system time. The system time is basically understandable as a weighted average out of the ensemble clocks. The stability can be assumed to be better than the best ensemble clock. Regarding the second requirement, “robustness,” the system time accepts loss of single clocks, which provides high reliability. Similar to the master concept, in order to meet the metrology requirement, the ensemble clocks are steered to UTC.

ENSEMBLE TIME: COMPOSITE CLOCK (CC)

The paper focuses on the timescale algorithm composite clock ([2-4]). It is a Kalman filter (KF) which models each ensemble clock by three states (Appendices A and B).

The Kalman filter is a recursive method which estimates the ensemble at time point t_k using the previous ensemble estimate and the measurement of time point t_k with $\tau := t_k - t_{k-1}$.

Assuming the ensemble consists out of N clocks, the inputs of the k -th Kalman filter iteration are

- $Z(t_k) \in R^{N-1}$ measurement w.r.t. measurement reference clock (MRC)
- $\hat{X}(t_{k-1}) \in R^{3N}$ previous ensemble estimate
- $C(t_{k-1}) \in R^{3N \times 3N}$ previous KF covariance.

Every KF-iteration can be separated into three steps. The first step is the prediction of the ensemble $\hat{X}^-(t_k) = \Phi \hat{X}(t_{k-1})$. Next, the measurement residual w.r.t. MRC is calculated:

$$\tilde{Z}(t_k) = Z(t_k) - H \Phi \hat{X}(t_{k-1})$$

with $H = H_{\#MRC} P$ (Appendix B). From KF-theory it is known that $\tilde{Z}(t_k)$ is a White and Gaussian process with zero mean ([14]). The conditional mean of the ensemble is calculated by

$$\hat{X}(t_k) = \Phi \hat{X}(t_{k-1}) + K(t_k) \tilde{Z}(t_k)$$

The corresponding Kalman gain is

$$K(t_k) = C^-(t_{k-1}) H^T (H C^-(t_{k-1}) H^T + R)^{-1}$$

with $C^-(t_{k-1}) = \Phi C(t_{k-1}) \Phi^T + Q(\tau)$.

Notice, the notation $\hat{X}(t_k) = (\hat{X}^{\#1}(t_k), \dots, \hat{X}^{\#N}(t_k))^T$ is used. $\hat{X}^{\#i}(t_k) \in R^3$ is the estimate of clock #i. Besides the ensemble estimate $\hat{X}(t_k)$ the iteration outputs the KF covariance

$$C(t_k) = C^-(t_{k-1}) - K(t_k)HC^-(t_{k-1}).$$

In detail, K. R. Brown developed several fundamental properties of the composite clock ([4]). A fundamental result is to understand the ensemble estimate w.r.t. to an implicitly defined system time $X^{ST}(t_k) \in R^3$

$$\hat{X}(t_k) = X(t_k) - \bar{H}X^{ST}(t_k) + N_{rep}(t_k) \quad (1)$$

with $\bar{H} := (I_3 \cdots I_3)^T \in R^{3N \times 3}$. $N_{rep}(t_k) \in R^{3N}$ is called representation error (to the implicit system time). The covariance of the representation error $C_{rep}(t_k) := Cov(N_{rep}(t_k))$ is

$$C_{rep}(t_k) = C(t_k) - \bar{H}(\bar{H}^T C^{-1}(t_k) \bar{H})^{-1} \bar{H}^T$$

[4]. A proof given by Brown shows that the KF estimates $\hat{X}(t_k)$ are unaffected using either $C_{rep}(t_k)$ or $C(t_k)$ (transparent variation). The advantage of $C_{rep}(t_k)$ compared to $C(t_k)$ is that its matrix entries converge which corresponds to the implicit steady state of the KF composite clock. However, the regular KF covariance $C(t_k)$ does not converge.

OPERATIONAL COMPOSITE CLOCK (OCC)

Although the Kalman filter composite clock is mathematically specified, its application in a real-world system results in several additional challenges on the CC. The stability of atomic clocks, which is modeled by the q-values (Appendix A), is not guaranteed for any time point. Clocks can be corrupted by different types of anomalies: time, frequency, or drift steps. Furthermore, the measurements can be disturbed by outliers. None of these anomalies is accurately modeled by the CC itself, thus corrupting the ensemble estimate.

The operational composite clock (OCC) is the extended version of the CC, which deals with operational issues of its real-world application.

OCC MODULE: INITIALIZATION

At the moment of the first available measurement $Z(t_1)$, no previous ensemble estimate $\hat{X}(t_0)$ and covariance $C(t_0)$ is available.

OPTION I: NO STATISTICAL INFORMATION

KF theory ([5-7]) recommends setting

$$\hat{X}(t_0) := E(X(t_0)) \text{ and } C(t_0) := Cov(X(t_0)).$$

It is a fundamental property of clock processes that the mean and covariance of $X(t_k)$ is unknown for any time point t_k . An option is to assume no statistical information about $X(t_0)$ and set $\hat{X}(t_0) := 0$ and to scale the corresponding clock covariance with a factor $l := (l_1 \ l_2 \ l_3)$:

$$q_i(\tau) := \begin{pmatrix} l_1 q_1 \tau + l_2 q_2 \frac{1}{3} \tau^3 + l_3 q_3 \frac{1}{20} \tau^5 & l_2 q_2 \frac{1}{2} \tau^2 + l_3 q_3 \frac{1}{8} \tau^4 & l_3 q_3 \frac{1}{6} \tau^3 \\ * & l_2 q_2 \tau + l_3 q_3 \frac{1}{3} \tau^3 & l_3 q_3 \frac{1}{2} \tau^2 \\ * & * & l_3 q_3 \tau \end{pmatrix}.$$

Plugging the $q_i(\tau)$ of the clocks together, the according ensemble process covariance is $Q_l(\tau)$ and $C(t_0) := Q_l(\tau)$. The initialization depends on the choice of l and is called option I.

OPTION II: PUT FIRST MEASUREMENT RESIDUAL TO ZERO

Using the properties of the measurement residual w.r.t. MRC

$$\tilde{Z}(t_1) = Z(t_1) - H\Phi\hat{X}(t_0)$$

a further initialization method can be derived. In an optimal designed KF, the measurement residual process shall be zero mean ([14]); thus, a reasonable choice is to put $\hat{X}(t_0) := \mu$ with

$$0 = Z(t_1) - H\Phi\mu. \quad (2)$$

The equation (2) is affine linear and the rank of $H\Phi$ is

$$rank(H\Phi) = N - 1$$

(without proof). The dimensional freedom of the solution is

$$\dim(\ker(H\Phi)) = 3N - rank(H\Phi) = 2N + 1.$$

An *ad-hoc* solution of equation (2) is to put clock # i with $i \neq MRC$

$$\hat{X}^{\#i}(t_0) := \mu^{\#i} := (Z_i(t_0) + a \ 0 \ 0)^T \text{ and } \hat{X}^{\#MRC}(t_0) := \mu^{\#MRC} := (a \ 0 \ 0)^T$$

with steer parameter “a.” Since the frequency and drift states are set to zero and the measurement residual is zero, there holds

$$\hat{X}(t_1) = \Phi \hat{X}(t_0) + K(t_1) \tilde{Z}(t_1) = \Phi \hat{X}(t_0) = \hat{X}(t_0)$$

for any starting covariance $C(t_0)$.

It remains a suitable choice of $C(t_0)$. Here, the authors are not sure. The applied option is to calculate offline the steady-state covariance

$$C_{rep}(t_\infty) := \lim_{k \rightarrow \infty} C_{rep}(t_k)$$

by successive iteration and put

$$C(t_0) := m C_{rep}(t_\infty)$$

The m parameter is used to scale the initial covariance.

OPTION III: PUT FIRST AND SECOND MEASUREMENT RESIDUALS TO ZERO

In option II, the initialization method puts the frequency states to zero. The method could run into trouble if the ensemble includes clocks with frequency offset. Typically, RAFS and SPHM have a deterministic drift, which leads to frequency offsets to the size of 1×10^{-12} or even more.

In order to properly initialize an ensemble including clocks with deterministic drift, option I is extended to use two measurement residuals. Set $\hat{X}(t_0) := \mu$ with

$$\begin{pmatrix} 0 \\ 0 \end{pmatrix} = \begin{pmatrix} Z(t_1) \\ Z(t_2) \end{pmatrix} - \begin{pmatrix} H\Phi \\ H\Phi\Phi \end{pmatrix} \mu \quad . \quad (4)$$

The equation (4) is again affine linear and the rank is

$$\text{rank} \begin{pmatrix} H\Phi \\ H\Phi\Phi \end{pmatrix} = 2(N-1)$$

(without proof).

As a result the dimensional freedom of the solution is

$$\dim(\ker \begin{pmatrix} H\Phi \\ H\Phi\Phi \end{pmatrix}) = 3N - 2(N-1) = N - 1 + 3.$$

The authors recommend uniquely solving the equation (4) by fixing the drift states of all clocks to zero and fixing one clock without frequency offset, e.g. $\mu^{\#MRC} := (0 \ 0 \ 0)^T$, to zero. The solution is called $\mu \in \mathbb{R}^{3N}$. Again, a control parameter a can be used to steer the time offset of the implicit system time. Setting $b^{\#i} := (a \ 0 \ 0)^T$ for every i , it holds that

$$b = (b^{\#1}, \dots, b^{\#N}) \in \ker \begin{pmatrix} H\Phi \\ H\Phi\Phi \end{pmatrix}$$

and $\mu + b$ solves the equation (4). The first and second ensemble estimates are

$$\hat{X}(t_1) = \Phi(\mu_u + b) \text{ and } \hat{X}(t_2) = \Phi\Phi(\mu_u + b).$$

In particular, $\hat{X}_1^{\#MRC}(t_1) = \hat{X}_1^{\#MRC}(t_2) = a$. Assuming the fundamental theorem of Brown, the arguments of option III holds and the implicit system time is steered in the same manner as presented in the example of option II. However, the steering quality depends on the representation error. Analogous to option II, the initial covariance is set to

$$C(t_0) := mC_{rep}(t_\infty).$$

EXAMPLE: INITIALIZING THE DLR CLOCK ENSEMBLE

The initialization options are compared using the ensemble of five atomic clocks operated at the DLR timing laboratory. The clock ensemble includes two high-performance HP cesium clocks (clock/cesium #1 and #3), one standard HP cesium clock (clock/cesium #2), a GPS-disciplined rubidium clock (clock #4), and an active hydrogen maser (clock #5/AHM) of KVARZ. The ensemble clocks are measured w.r.t. to clock #5 using a time-interval counter.

The outlined options I, II, and III are investigated with $m = 2$ (option II and III), $l = (1 \times 10^{20}, 1 \times 10^{10}, 1 \times 10^{10})$ (option I) and $a = 0$ (option I/II/III) to initialize the ensemble.

Figure 2 and 3 show the 2nd-state estimates of the cesium #1 and the AHM for all options. In Figure 1, the 2nd-state estimates are biased around 1×10^{-13} for option I and III. The option III is shifted about 0.5×10^{-13} .

Similar, the 2nd-state estimates of the AHM are biased between 6×10^{-14} and 10×10^{-14} in the case of option I and III. The bias of option II is around 1×10^{-14} .

Assuming that the clocks are free of a frequency offset, option II consistently estimates the clocks. It is the most promising initialization method in this situation.

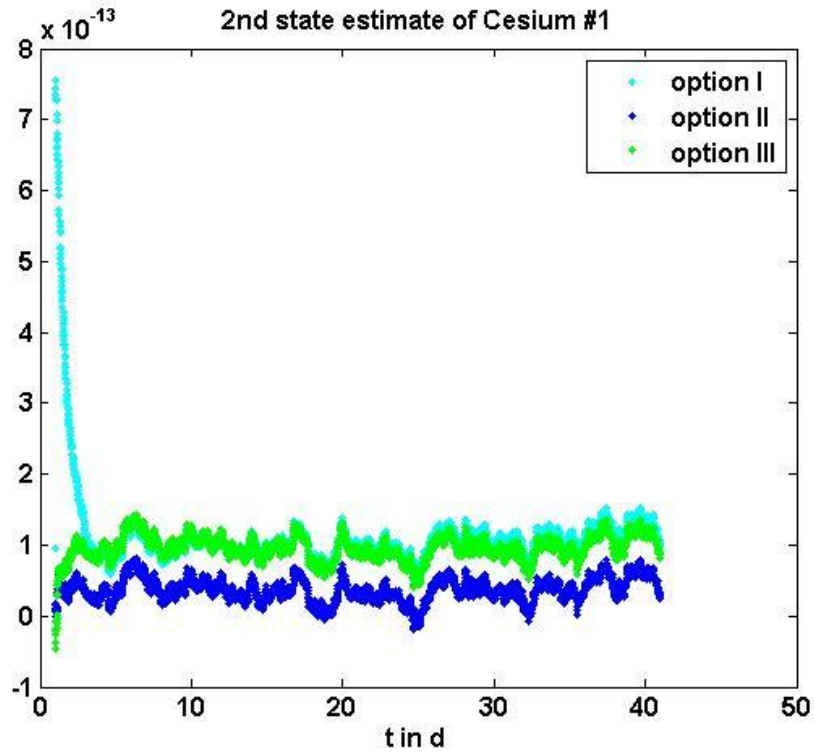


Figure 1. 2nd-state estimate of Cesium #1.

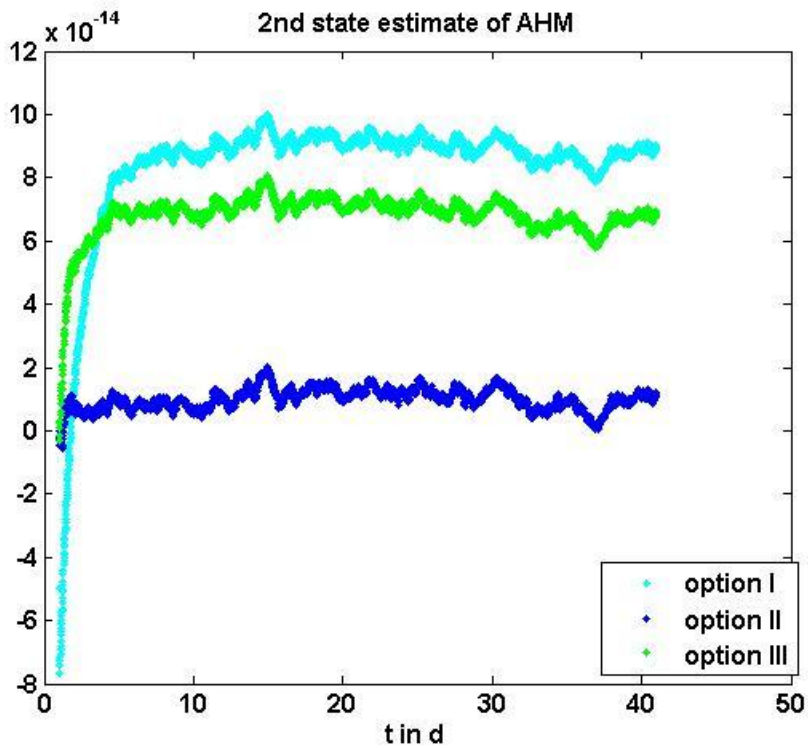


Figure 2. 2nd-state estimate of AHM.

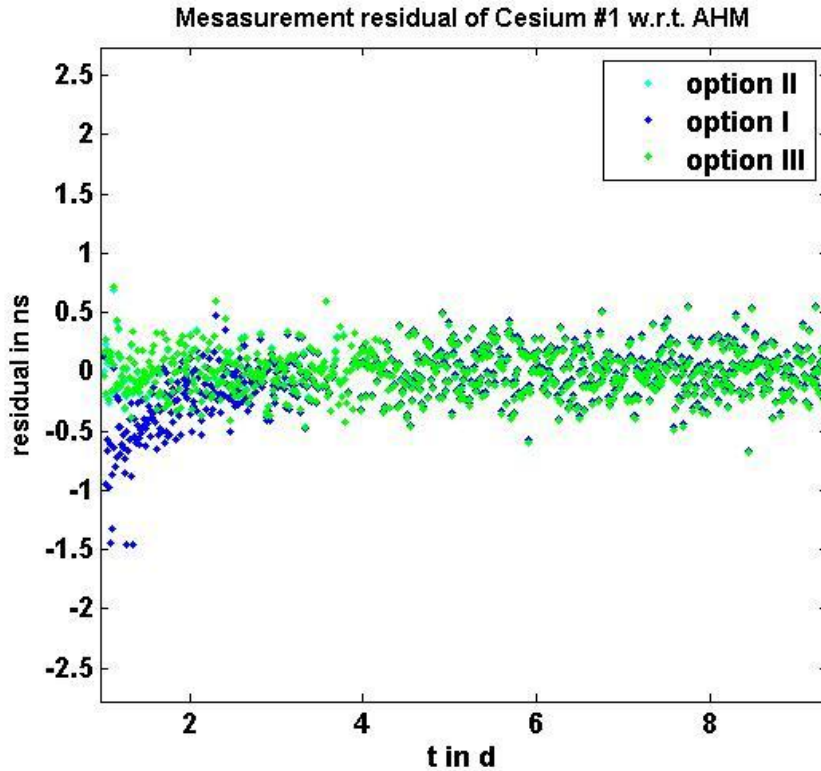


Figure 3. Measurement residual of Cesium #1 w.r.t. AHM.

Figure 3 shows the corresponding measurement residuals of Cesium #1 w.r.t. to AHM. By visual check, the residuals of option I are biased till the day two. The residuals of option II and III are almost identical and unbiased from the beginning.

OCC MODULE: IDENTIFICATION OF NON- AND ACTIVE CLOCKS

The k -th iteration processes the measurement $Z(t_k)$ to compute the actual ensemble estimate based on the former estimate $\hat{X}(t_{k-1})$. $Z(t_k)$ can be corrupted by outlier, time step, non-available measurement or frequency steps. None of these anomalies is modelled by the Kalman filter; thus, a regular processing of a corrupted measurement likely disturbs the ensemble estimate. It is the fundamental task of the consistency check to detect such kinds of anomalies in order to provide the robustness requirement of the OCC.

CONSISTENCY CHECK OF MEASUREMENTS

The statistics of the measurement residual w.r.t. MRC

$$\tilde{Z}(t_k) = Z(t_k) - H\Phi\hat{X}(t_{k-1})$$

is applied to do a consistency check of the residual ([2]). The covariance of $\tilde{Z}(t_k)$ is

$$HC^-(t_k)H^T + R = HC_{rep}^-(t_k)H^T + R.$$

A hypothesis test of each component of $\tilde{Z}(t_k)$ is performed ([2]). Clock #i is called *active* w.r.t. MRC, if

$$|\tilde{Z}_i(t_k)| < 4\sqrt{\left(HC_{rep}^-(t_k)H^T + R\right)_{i,i}}.$$

Otherwise, it is called *non-active* w.r.t. MRC.

It remains to test the measurement reference clock. The authors employ an *ad-hoc* method. In the case of less than two active clocks w.r.t. MRC, the measurement reference clock is called non-active and active, vice-versa. By definition, a clock whose measurement is not available is called non-active, too.

CONSISTENCY CHECK OF RE-REFERENCED MEASUREMENTS

In case the measurement reference clock is identified as non-active, the measurement residual is not $\tilde{Z}(t_k)$ processed and an alternate reference clock is determined.

The measurements are re-referenced to a so-called trial reference clock #l:

$$\begin{aligned} Z_i^{\#l}(t_k) &:= Z_i(t_k) - Z_l(t_k) = X_1^{\#i}(t_k) - X_1^{\#MRC}(t_k) + V_i(t_k) - (X_1^{\#l}(t_k) - X_1^{\#MRC}(t_k) + V_l(t_k)) \\ &= X_1^{\#i}(t_k) - X_1^{\#l}(t_k) + V_i(t_k) - V_l(t_k) \\ \cdot Z_{MRC}^{\#l}(t_k) &:= -Z_l(t_k) = X_1^{\#MRC}(t_k) - X_1^{\#l}(t_k) - V_l(t_k). \end{aligned}$$

By adapting the measurement matrix to $H^{\#l} := H_l P$ (Appendix B), a hypothesis test of the measurement residual w.r.t. to trial reference clock #l

$$\tilde{Z}^{\#l}(t_k) := Z^{\#l}(t_k) - H^{\#l} \Phi \hat{X}(t_{k-1})$$

is performed:

$$\left|\tilde{Z}^{\#l}(t_k)\right|_{i,i} < 4\sqrt{\left(H^{\#l}C_{rep}^-(t_k)(H^{\#l})^T + 2R\right)_{i,i}}.$$

The same method to separate non-active and active clocks is executed as in the case of the measurement reference clock.

Performing a consistency check w.r.t. to every ensemble clock, a so-called *consistency matrix* is computed. The i-th row indicates the applied trial reference clock #i and the j-th column indicates the

measurement residual of clock #j. The matrix entry with index (i,j) is set to 1, if the consistency check of clock #i w.r.t. to trial reference #j is consistent, and zero otherwise.

OCC MODULE: KALMAN FILTER ADAPTATION

The consistency matrix is used to determine the so called Kalman filter reference clock (KRC). In case the entry of the measurement reference clock is 1, it is used as KRC. Otherwise, a clock with diagonal entry “1” is selected as KRC. The corresponding row vector determines the active clocks (having “1” entries). The measurement and measurement matrix are adapted in a way that the non-active clocks are excluded. Furthermore, the measurement matrix is adapted w.r.t. KRC. In case no valid KRC can be identified, the ensemble estimate and covariance are predicted.

Since the number of active clocks M can be less than N , the former ensemble estimate $\hat{X}(t_{k-1})$ and KF covariance $C_{rep}(t_{k-1})$, which are of dimension $3N$ and $(3N,3N)$, are adopted. The non-active clocks are excluded from the former estimate $\hat{X}(t_{k-1})$ to define $\hat{M}(t_{k-1}) \in R^{3M}$.

The covariance adaptation distinguishes two cases. In the first case, the number of active clocks at t_k compared to t_{k-1} decreases. The row and columns of the non-active clocks are excluded from the former covariance $C_{rep}(t_{k-1})$ to define $P(t_{k-1}) \in R^{3M \times 3M}$.

In the second case, the number of active clocks increases. $C_{rep}(t_{k-1})$ is reset to the steady of all clocks (offline computation). Afterwards, the rows and columns of the non-active clocks are excluded to define $P(t_{k-1}) \in R^{3M \times 3M}$. The authors observe by simulation that if the number of active clocks increases, the covariance does not reach the steady state reusing the previous $C_{rep}(t_{k-1})$. That is the reason to reset $C_{rep}(t_{k-1})$ to the steady state of all clocks and exclude the non-active clocks. The reduced covariance converges.

The actual estimate $\hat{M}(t_k)$ and covariance $P(t_k)$, using transparent variation, is computed based on $\hat{M}(t_{k-1})$ and $P(t_{k-1})$.

It remains to set $C_{rep}(t_k) \in R^{3N \times 3N}$. Consequently, the rows and columns of the active clocks of $C_{rep}(t_k)$ are set to the corresponding ones of $P(t_k)$. The non-active clocks are set to the corresponding ones of $C_{rep}(t_{k-1})$.

Notice, the entries $C_{rep}(t_k)$ of the non-active clocks are modified, if the number of active clocks increases. In this situation, the number of active decreases and some entries are unmodified.

OCC MODULE: NON-ACTIVE CLOCK CALCULATION

It remains a procedure to calculate the non-active clocks w.r.t. to the implicit system time. The procedure depends on the reason of on non-activeness.

NO MEASUREMENT AVAILABLE

In case of a non-available measurement, the non-active clock #i is predicted: $\hat{X}^{\#i}(t_k) := \phi \hat{X}^{\#i}(t_{k-1})$.

CONSISTENCY FAILURE

In case the clock is non-active due to violating the consistency check, the procedure depends on the consistency of iteration t_{k-1} . If the clock is previously active, the non-active clock #i is predicted: $\hat{X}^{\#i}(t_k) := \phi \hat{X}^{\#i}(t_{k-1})$. It is assumed that the consistency check fails because of an outlier. If it was previously non-active, the time offset w.r.t. the implicit system time is calculated using $\hat{X}_1^{\#KRC}(t_k)$ and $Z_i^{\#KRC}(t_k)$:

$$\begin{aligned} Z_i^{\#KRC}(t_k) + \hat{X}_1^{\#KRC}(t_k) &= X_1^{\#i}(t_k) - X_1^{\#KRC}(t_k) + V_i(t_k) + (X_1^{\#KRC}(t_k) - X_1^{ST}(t_k) + N_1^{\#KRC}(t_k)) \\ &= X_1^{\#i}(t_k) - X_1^{ST}(t_k) + V_i(t_k) + N_1^{\#KRC}(t_k) =: \hat{X}_1^{\#i}(t_k). \end{aligned}$$

The second and third states of clock #i are predicted:

$$\hat{X}_2^{\#i}(t_k) := \hat{X}_2^{\#i}(t_{k-1}) + \tau \hat{X}_3^{\#i}(t_{k-1}) \text{ and } \hat{X}_3^{\#i}(t_k) := \hat{X}_3^{\#i}(t_{k-1}).$$

OVERVIEW OF OPERATIONAL COMPOSITE CLOCK (OCC)

Figure 4 shows the work flow of the Operational Composite Clock.

ROBUSTNESS AND STABILITY OF DLR'S OCC

The DLR clock ensemble of 5 atomic clocks (example: initialization) is processed using the OCC.

HANDLING OF OUTLIERS AND TIME STEPS

Figure 5 shows the measurement of Cesium #3 w.r.t. AHM. It is corrupted by several outliers, and a time step occurs at $t = 68.74d$. Focusing on the measurement residual of Cesium #3 w.r.t. AHM (Figure 6), the outliers and the time step can be visually identified and are detected by the OCC consistency check module.

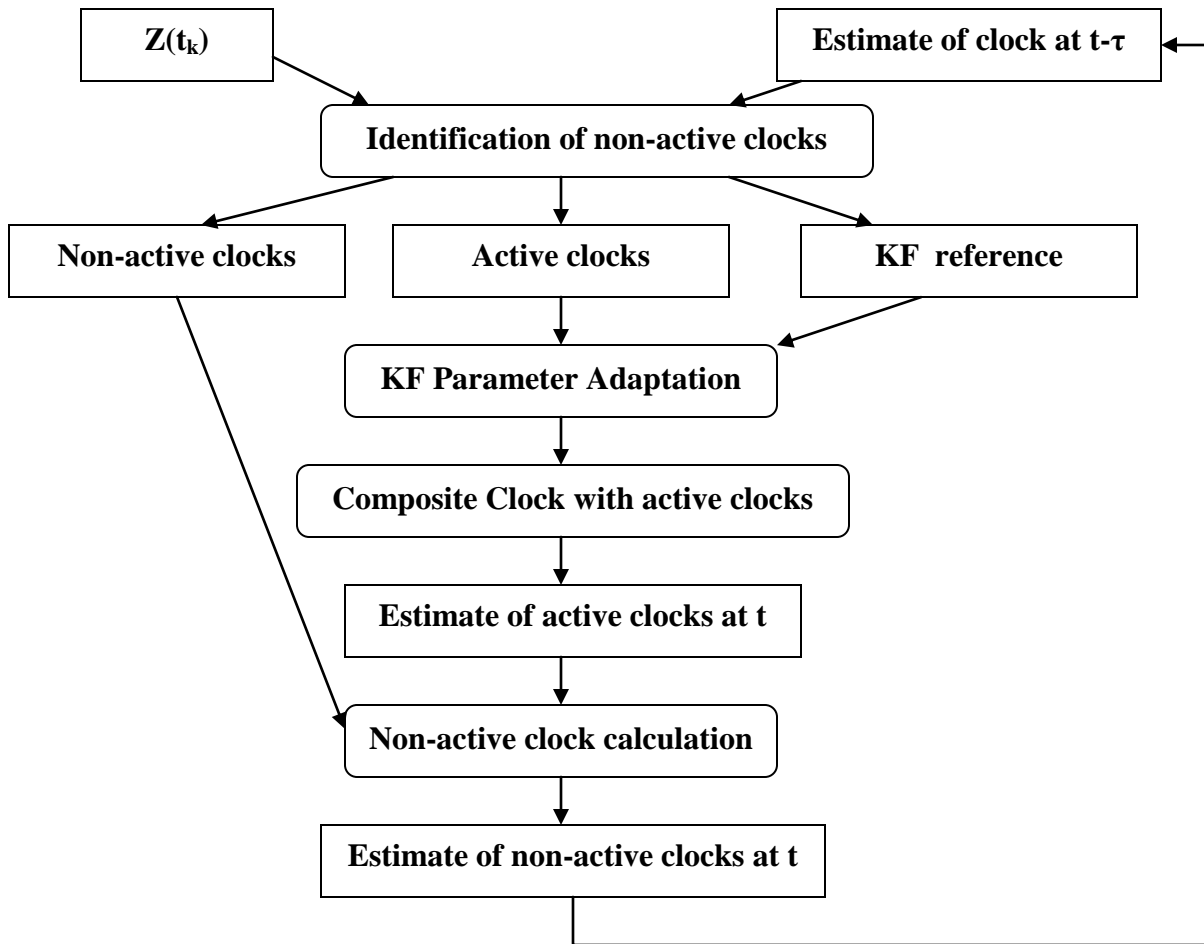


Figure 4. Work flow of Operational Composite Clock.

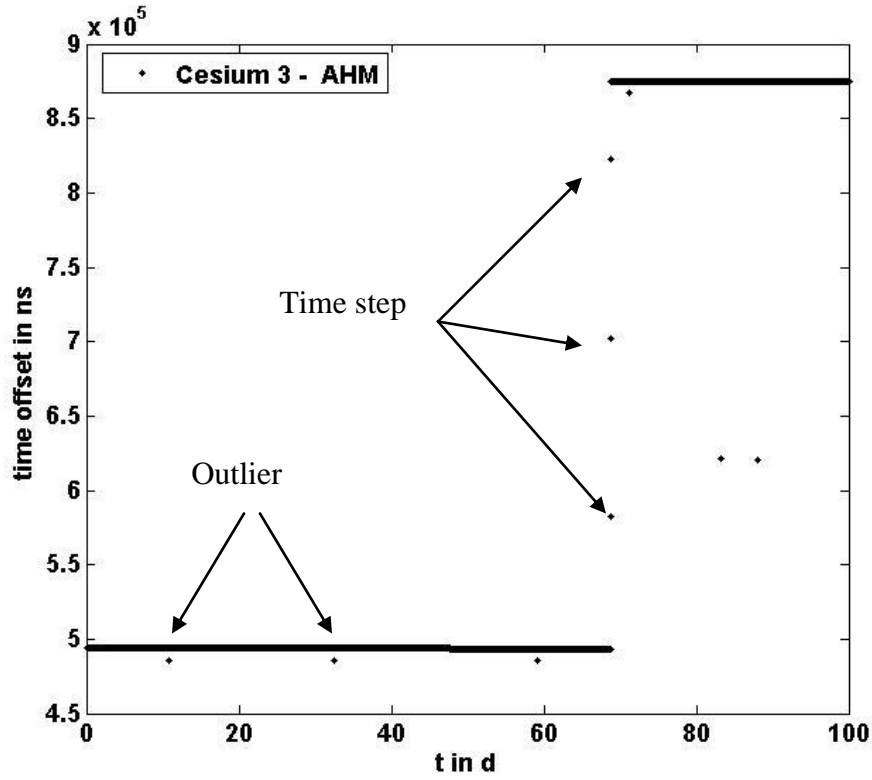


Figure 5. Measurement of Cesium #3 w.r.t. AHM.

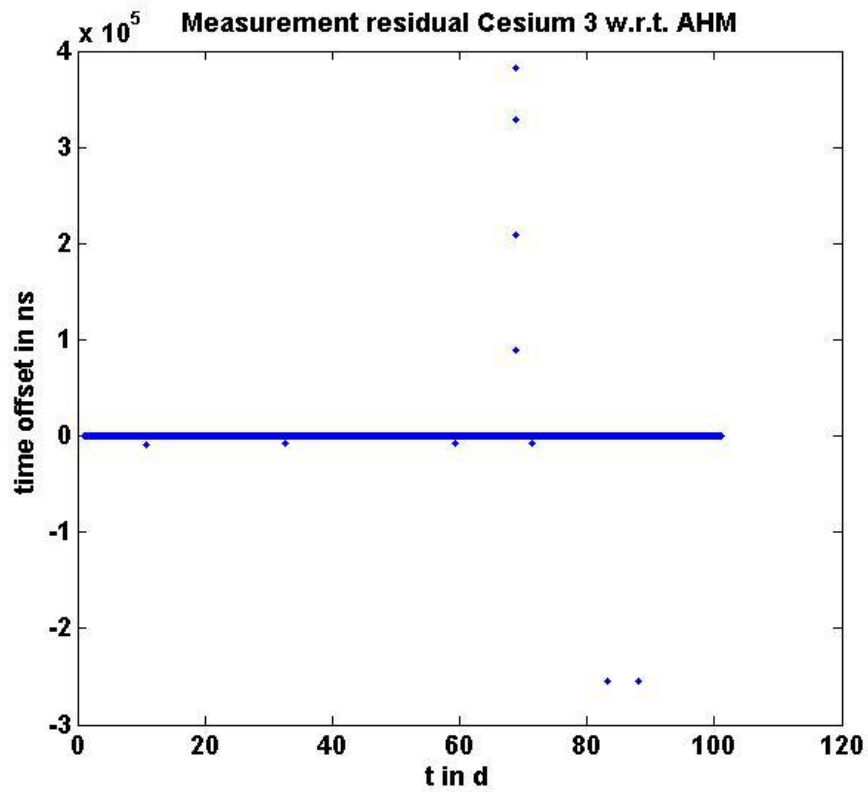


Figure 6. Measurement residual of Cesium #3 w.r.t. AHM.

In case of the outliers the estimate of the Cesium #3 corresponds to its prediction (Figure 7). However, to deal with the time step at $t = 68.74\text{d}$, several steps are executed by the OCC. As outlined, the consistency matrix is used to choose a valid KF reference clock. At $t = 68.74\text{d}$, no valid KRC can be identified; thus, the ensemble is predicted. The same enters the following two iterations. Analyzing the fourth iteration after $t = 68.74\text{d}$, the diagonal entry of the AHM is still zero and set to non-active. The remaining diagonal entries are 1 and can be used as KF reference clock. The time step of the AHM is finally present in every clock measurement; thus, it is dropped out by the re-referencement method. It remains in the AHM measurement residual w.r.t. to the trial reference clock and, thus, the AHM is set to non-active w.r.t. the trial reference clock.

The OCC module KF parameter adaptation excludes the AHM and set the KF reference. The remaining active clocks are estimated. Figure 4 shows the estimate of Cesium #3 – it is not impacted by the time step.

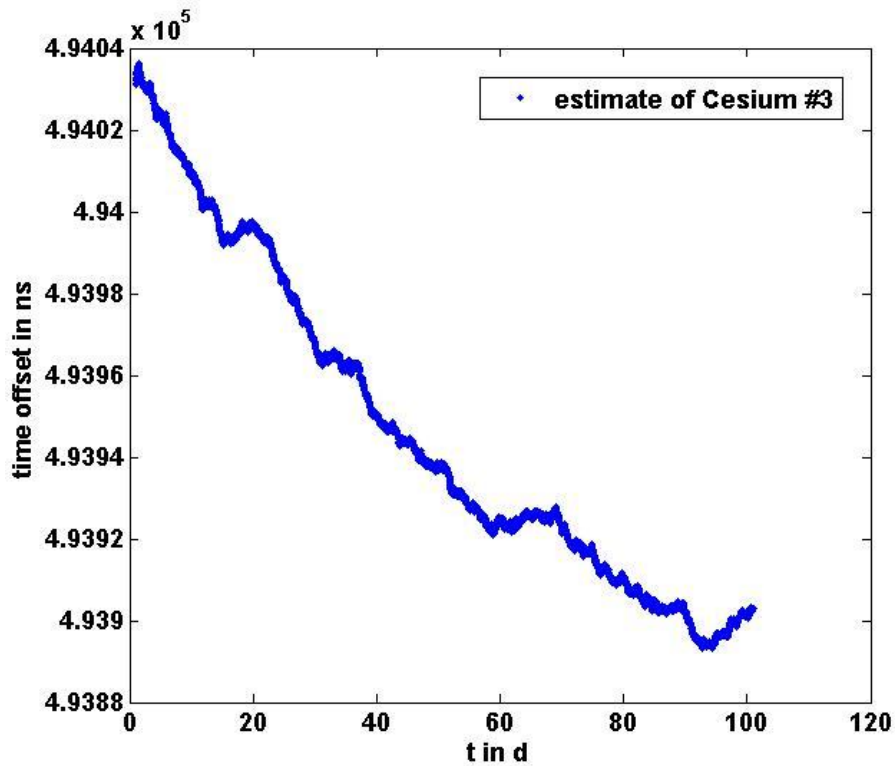


Figure 7. First state estimate of Cesium #3.

Contrarily, the estimate of AHM includes the time step of the AHM (Figure 8).

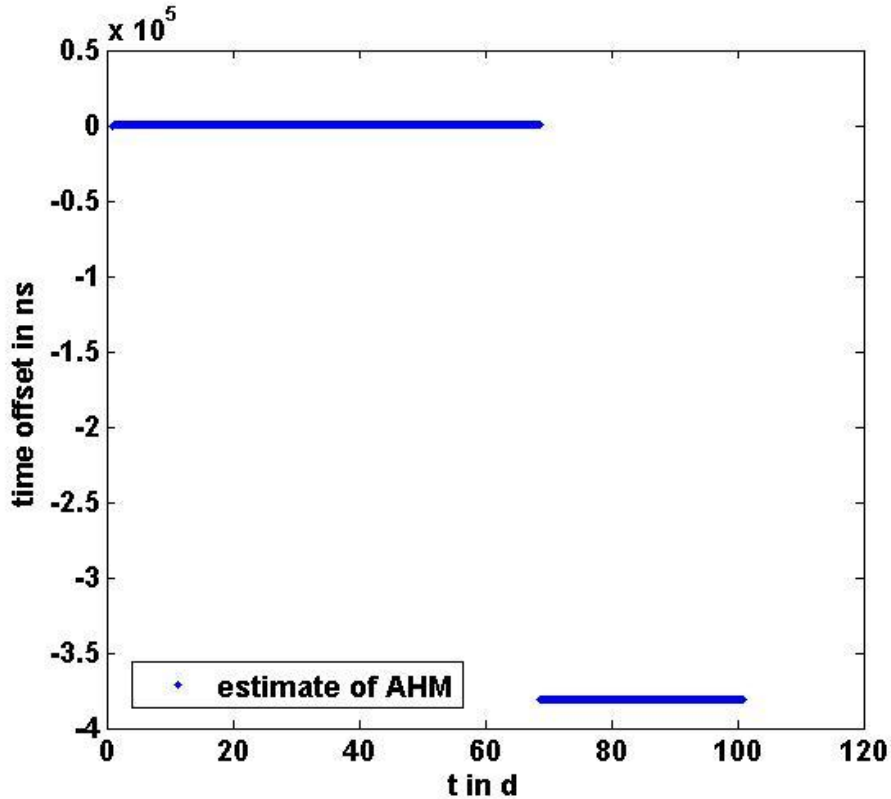


Figure 8. First state estimate of AHM.

ALLAN DEVIATION OF TIME LAB CLOCKS

Both the KF estimates as well as the measurements are corrupted by anomalies; thus, the empirical Allan deviation of the data is impacted, having no exclusion method. The Dynamic Allan deviation ([15]) can be used to handle this issue in another way. At each time point t_k , the Allan deviation is calculated using a fixed window of data. Data windows, free of anomalies, are used to calculate the Allan deviation of the clocks.

The time-interval counter is specified with $2 \cdot 10^{-11} \tau^{-1}$. Figure 9 compares the stabilities of the Cesium #1 w.r.t. AHM or the implicit system time. The stability of the Cesium #1 estimate and the measurement w.r.t. AHM are almost identical. This indicates that neither the AHM nor the implicit system time impact the stability of Cesium #1. Its performance is extrapolated as $6 \cdot 10^{-12} \tau^{-0.5}$, worse than its hardware specification of $5 \cdot 10^{-12} \tau^{-0.5}$.

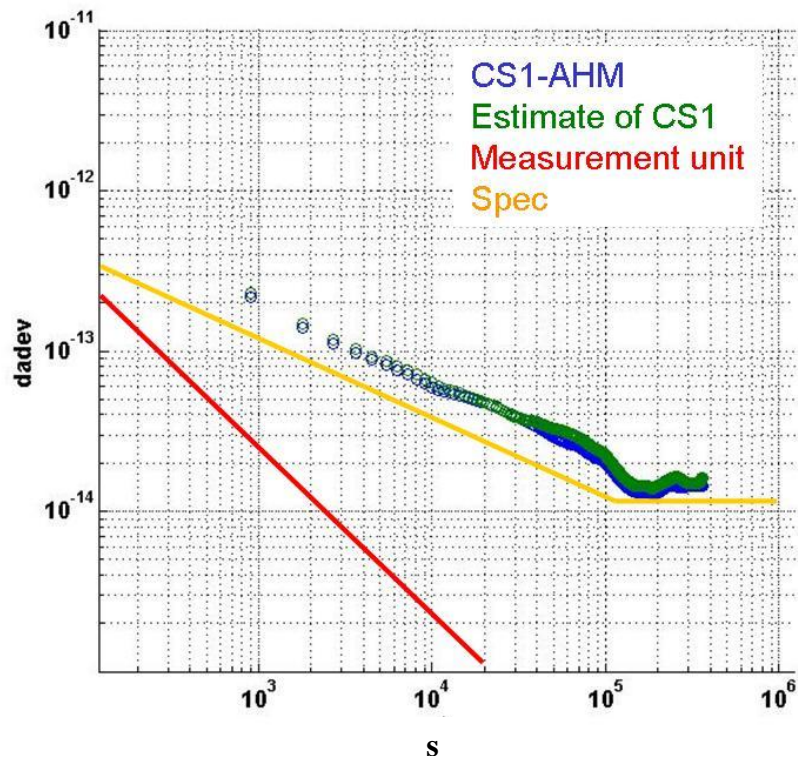


Figure 9. Stabilities of high performance Cesium #1.

Figure 10 shows the stability of the AHM estimate. Its stability is extrapolated as $1 \cdot 10^{-12} \tau^{-0.5}$, worse than its specification of $2 \cdot 10^{-13} \tau^{-0.5}$. This is reasoned because the cesium clocks are part of the implicit system time. The stability of the weighted cesium clocks is worse than the stability of the AHM. As a result, the stability of the AHM estimate is characterized by the weighted cesium clock stability.

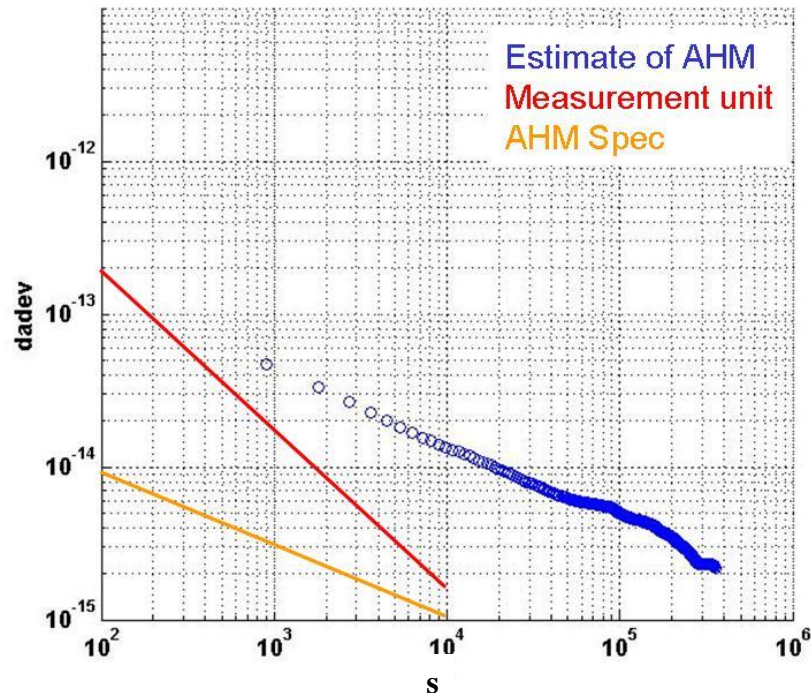


Figure 10. Stability of AHM.

CONCLUSION

The paper describes required methods to operate the composite clock in a real-world environment (Time-lab, GNSS). The statistic properties of the measurement residual process, which is a zero mean and Gaussian process (KF theory), are utilized to develop consistent initialization procedures. The recommended initialization procedure puts the ensemble state in a way to solve the measurement residual equation for either one or two measurement residuals. Testing the procedure with a DLR clock ensemble of five atomic clocks, the most promising results for that ensemble are achieved by fixing the frequency states as well as the drift states to zero. However, initializing a clock ensemble including clocks with frequency offsets it is recommended to solve the measurement residual equation using two measurement residuals. As a result, frequency estimates of the clock ensemble are provided.

Based on the measurement residual process, a hypothesis test is described which splits the ensemble in active and non-active clocks. The hypothesis test works with any reference clock as long as it is part of the ensemble. The Kalman filter is executed with the active clocks to calculate estimates of them. The non-active clocks are calculated using an additional method. The robustness of the OCC is validated using measurements out of the DLR clock laboratory. Outliers along with time steps of the reference clock are detected and processed by the OCC without disturbing the remaining estimates.

ACKNOWLEDGMENTS

The authors would like to say thank you to Demetrios Matsakis (USNO) for helpful and useful comments on the paper.

APPENDICES

A: CLOCK AND ENSEMBLE PROCESS

The process of clock #i is defined by ([4,9,16,17]):

$$X^{\#i}(t_k) = \phi X^{\#i}(t_{k-1}) + W^{\#i}(t_k)$$

with $\phi = \begin{pmatrix} 1 & \tau & 0.5\tau^2 \\ 0 & 1 & \tau \\ 0 & 0 & 1 \end{pmatrix}$. $W^{\#i}(t_k)$ is a White and zero mean Gaussian process with

$$Cov(W^{\#i}(t_k)) = Q^{\#i}(\tau) = \begin{pmatrix} q_1\tau + q_2\frac{1}{3}\tau^3 + q_3\frac{1}{20}\tau^5 & q_2\frac{1}{2}\tau^2 + q_3\frac{1}{8}\tau^4 & q_3\frac{1}{6}\tau^3 \\ * & q_2\tau + q_3\frac{1}{3}\tau^3 & q_3\frac{1}{2}\tau^2 \\ * & * & q_3\tau \end{pmatrix}. \quad (q_1, q_2, q_3)\text{-value is the so-}$$

called q-value. Correspondingly, the ensemble and noise processes are defined by $X(t_k) = (X^{\#1}(t_k), \dots, X^{\#N}(t_k))^T$ and $W(t_k) = (W^{\#1}(t_k), \dots, W^{\#N}(t_k))^T$. $W^{\#1}(t_k), \dots, W^{\#N}(t_k)$ are stochastically independent and

$$Q(\tau) = Cov(W(t_k)).$$

It is $\Phi = I_N \otimes \phi$.

B: MEASUREMENT PROCESS

Define the matrix

$$P = \begin{pmatrix} 1 & 0 & 0 & \dots & \dots & \dots & \dots & 0 \\ 0 & 0 & 0 & 1 & 0 & 0 & \dots & 0 \\ \vdots & \ddots & \ddots & \ddots & \ddots & \ddots & \ddots & \vdots \\ 0 & \dots & \dots & \dots & \dots & 1 & 0 & 0 \end{pmatrix} \in R^{N \times 3N}$$

and

$$H_r = \begin{pmatrix} e_1 - e_r \\ e_2 - e_r \\ \vdots \\ e_{r-1} - e_r \\ e_{r+1} - e_r \\ \vdots \\ e_N - e_r \end{pmatrix} \in R^{(N-1) \times N}$$

with $e_i \in R^N$ i-th unit vector and measurement reference clock #r. The measurement process is defined by

$$Z(t_k) = H_r P X(t_k) + V(t_k)$$

with $V(t_k) = (V_1(t_k) \ \cdots \ V_{N-1}(t_k))^T$ and $Cov(V(t_k)) = R$. The measurement matrix is defined by $H = H_r P$.

REFERENCES

- [1] P. Tavella and C. Thomas, 1991, "Comparative Study of Time Scale Algorithms," **Metrologia**, **28**, 57-63.
- [2] R. Jones and P. Tryon, 1983, "Estimating Time From Atomic Clocks," **Journal of Research of the National Bureau of Standards**, **88**, 17-24.
- [3] P. Tryon and R. Jones, 1983, "Estimation of Parameters in Models for Cesium Beam Atomic Clocks," **Journal of Research of the National Bureau of Standards**, **88**, 3-16.
- [4] K. R. Brown, 1991, "The Theory of the GPS Composite Clock," in Proceedings of the 4th International Technical Meeting of the Satellite Division of the Institute of Navigation (ION GPS), 11-13 September 1991, Albuquerque, New Mexico (Institute of Navigation, Alexandria, Virginia), pp. 223-241.
- [5] A. H. Jazwinski, 2007, **Stochastic Processes and Filtering Theory** (Dover, New York).
- [6] P. S. Maybeck, 1979, **Stochastic Models, Estimation and Control** (Academic Press, Burlington, Massachusetts).
- [7] M. Grewal and A. P. Andrews, 1993, **Kalman Filtering – Theory and Practice** (Prentice-Hall, Englewood Cliffs, New Jersey).
- [8] R. H. Shumway, D. E. Olsen, and L. J. Levy, 1981, "Estimation and tests of hypotheses for the initial mean and covariance in the Kalman filter model," **Communications in Statistics - Theory and Methods**, 10.

- [9] S. T. Hutsell, 1996, “*Relating the Hadamard Variance To MCS Kalman Filter Clock Estimation,*” in Proceedings of the 27th Annual Precise Time and Time Interval (PTTI) Systems and Applications Meeting, 29 November-1 December 1995, San Diego, California, USA (NASA CP-3334), pp. 291-301.
- [10] S. T. Hutsell, 1995, “*Fine Tuning GPS Clock Estimation in the MCS,*” in Proceedings of the 26th Annual Precise Time and Time Interval (PTTI) Systems and Applications Meeting, 6-8 December 1994, Reston, Virginia, USA (NASA CP-3302), pp. 63-74.
- [11] S. T. Hutsell, 1994, “*Recent MCS Improvements to GPS Timing,*” in Proceedings of ION GPS-94 (Institute of Navigation, Alexandria, Virginia), pp. 261-273.
- [12] S. T. Hutsell, 1996, “*Ideas For Future GPS Timing Improvements,*” in Proceedings of the 27th Annual Precise Time and Time Interval (PTTI) Systems and Applications Meeting, 29 November-1 December 1995, San Diego, California, USA (NASA CP-3334), pp. 63-74.
- [13] K. R. Brown, M. Chien, W. Mathon, S. Hutsell, and C. Shank, 1995, “*L-Band Anomaly Detection in GPS,*” in Proceedings of the 51st Annual Meeting of ION, 5-7 June 1995, Colorado Springs, Colorado, USA (Institute of Navigation, Alexandria, Virginia), pp. 107-117.
- [14] R. K. Mehra, 1970, “*On the Identification of Variances and Adaptive Kalman Filtering,*” **IEEE Transactions on Automatic Control**, **AC-15**, 175-184.
- [15] L. Galleani and P. Tavella, 2008, “*Detection and identification of atomic clock anomalies,*” **Metrologia**, **45**, 127-133.
- [16] C. Zucca and P. Tavella, 2005, “*The clock model and its relationship with the Allan and related variances,*” **IEEE Transactions on Ultrasonics, Ferroelectrics, and Frequency Control**, **UFFC-52**, 289-296.
- [17] J. W. Chaffee, 1987, “*Relating the Allan Variance to the Diffusion Coefficients of a Linear Stochastic Differential Equation Model for Precision Oscillators,*” **IEEE Transactions on Ultrasonics, Ferroelectrics, and Frequency Control**, **UFFC-34**, 655-658.